Tribology International xxx (xxxx) 110766

Contents lists available at ScienceDirect

Tribology International

journal homepage: www.elsevier.com/locate/triboint

Enhancing the shredder durability for biomass preprocessing by utilizing wear-resistant cutter materials

Tomas Grejtak [a,*], Miranda W. Kuns [b], Jeffrey A. Lacey [c], Oyelayo O. Ajayi [d], George Fenske [d], Peter J. Blau [e], Jun Qu [a,*]

[a] Materials Science and Technology Division, Oak Ridge National Laboratory, 1 Bethel Valley Road, Oak Ridge, TN 37831, United States
[b] Biological and Chemical Processing Department, Idaho National Laboratory, 1955 Fremont Ave, Idaho Falls, ID 83415, United States
[c] Engineering Process Design and Realization Department, Idaho National Laboratory, 1955 Fremont Ave, Idaho Falls, ID 83415, United States
[d] Applied Materials Division, Argonne National Laboratory, 9700 South Cass Avenue, Lemont, IL 60439, United States
[e] Blau Tribology Consulting, 626 Wickhams Fancy Drive, Candler, NC 28715, United States

ARTICLE INFO

Keywords:
Biomass
Cutter wear
Surface treatment
Tool steel

ABSTRACT

Shredders are widely used to reduce biomass feedstock size through the shearing action of the cutter teeth that are susceptible to wear. A series of wear tests using a custom-built shredder was conducted on corn stover feedstock with three cutter materials: a conventional D2 tool steel, iron boriding as a candidate surface treatment, and M42 tool steel as a candidate alloy. Wear tests showed that the iron borided D2 steel significantly increased the tool life compared with the non-treated D2 and M42. Although the M42 cutters initially exhibited less wear than the D2 cutters, the benefit faded as preprocessing progressed. The experimental results demonstrated that the durability of shredder cutters can be substantially improved by applying more wear-resistant tool materials.

1. Introduction

Size reduction of biomass is an essential preprocessing step for enhancing the efficiency of biomass, biofuel, and biochemical production [1,2]. Raw lignocellulosic biomass is significantly larger than the particle sizes required for bioprocessing, which typically range from 0.2 to 10 mm, depending on the application. For example, at the lower range, the biomass size requirement for pelletizing is 0.6–0.9 mm [3,4], and pyrolysis requires 0.2–2.0 mm [5,6]. In applications such as briquetting or fermentation, the size of the biomass particles can be larger: up to 5 mm [7] and 10 mm [8], respectively.

Biomass size can be reduced by using various comminution systems such as specialized mills or shredders, depending on the biomass type, desired particle size, and other characteristics [1,2]. In knife mills, the biomass is sheared and cut via the interaction between rotating and stationary knives, allowing for improved particle flowability and narrower size distribution [9,10]. Hammer mills use rotating hammers to pulverize biomass. This technique can be applied to a wide range of feedstock types; however, they are not suitable for high-moisture biomass [11,12]. By contrast, in a rotary shear, a special type of shredders, the biomass is captured, pulled in, and then torn, sheared, and crushed (i.e., shredded) by the cutters [2,13]. This technique can accommodate high-moisture biomass, but it cannot reduce the size of the particles below 1 mm [13].

One of the challenges facing biomass preprocessing equipment is excessive wear of the tooling components [2,9,12,14,15]. Biomass feedstock contains inorganic particles commonly known as ash, which either can be introduced to the feedstock through soil contamination during harvesting or can be contained within plant cells [14–17]. Characterization of the biomass ash by Lee et al. [16] showed that these inorganics are tens to hundreds of micrometers in size, primary composed of quartz and are considerably harder than the steel components used in preprocessing tooling. Undesirable wear and damage to the tooling components can eventually lead to increased costs in biomass preprocessing, lower feedstock throughput, irregular particle size of the processed feedstock and higher power consumption of the preprocessing equipment [9].

Several studies investigated the wear mechanism of biomass preprocessing equipment. For example, significant effort has focused on a rotary bypass shear mill (Crumbler) developed by Forest Concepts, LLC [13,18–20]. A study by Lee et al. [13] showed that the dominant wear mode of cutters in the rotary shear mill is a two-body and three-body abrasion owing to their rubbing against softer biomass and the harder external inorganic contaminates. Fenske et al. [18] developed an analytical model to predict wear of the cutters during contact with hard,

* Corresponding author at: Materials Science and Technology Division, Oak Ridge National Laboratory, Oak Ridge, TN 37831, USA.
E-mail addresses: grejtakt@ornl.gov (T. Grejtak), qujn@ornl.gov (J. Qu).

https://doi.org/10.1016/j.triboint.2025.110766
Received 10 January 2025; Received in revised form 29 April 2025; Accepted 1 May 2025
0301-679/© 20XX

CORRECTED PROOF

Note: Low-resolution images were used to create this PDF. The original images will be used in the final composition.

abrasive silica particles. Finite Element Analysis (FEA) by Lin et al. [20] simulated contact stresses generated on a cutter as a function of silica particle size and shape. In another study by Lin et al., FEA was used to optimize the design of clearing plates to improve the flow of the processed feedstock and to reduce the contact stresses from interaction with silica particles [19]. The wear mechanism of a hammer mill was studied by Roy et al. [12]. The study showed that the impact and sliding of hammers against biomass and contaminants causes their erosion and polishing wear.

Wear of the tooling components of the biomass preprocessing equipment can be mitigated by applying advanced wear-resistant materials. Also, specialized surface treatments such as boriding, chromizing, carburizing, or nitriding [21] and coatings such as WC-Co, SiC, or diamond-like carbon coating [22] are commonly used to improve the wear resistance and hardness of ferrous materials. In a study by Grejtak et al. [9], full-scale knife mill experiments were conducted for the size reduction of pine forest residue feedstock using three types of knife materials: candidate iron borided tool steel, WC-Co insert, and a conventional tool steel as a baseline. The knife mill experiments clearly showed that the boriding surface treatment and WC-Co insert improved the wear resistance of the knives by 3 and 8 times, respectively, which led to increased throughput and reduced power consumption during knife mill operation. Furthermore, a techno-economic analysis (TEA) demonstrated that using these advanced, more wear-resistant knife materials reduced downtime by 65 %–85 %, due to less frequent knife replacement. The application of these materials also lowered the milling cost by $2–$3 per ton of processed feedstock.

The cutters in shredders for biomass preprocessing are commonly made of tool steels and, like those in knife mills, are subject to excessive wear when processing dirty biomass feedstocks. The objective of this work was to demonstrate that the durability of shredder cutters can be enhanced by applying more wear-resistant tool materials. Three shredder wear tests were conducted, each using a different cutter material: a D2 tool steel as the baseline, iron borided D2 tool steel as candidate surface treatment, and a M42 tool steel as a candidate alloy. The cutter performance was evaluated based on the measured cutter tooth length recession. The cutters' worn surfaces were characterized to determine and compare the wear modes of the tested cutter materials. The outcomes of this work could be applied to enhance the wear resistance and durability of tooling components in various biomass preprocessing equipment.

2. Materials and methods

2.1. Cutter materials

Three cutter materials were selected for the shredder wear testing: iron borided D2 tool steel as a candidate surface treatment, M42 tool steel as the candidate wear resistant alloy, and D2 tool steel as the baseline. High-carbon steels and tool steels are commonly used as cutter material in applications such as shredders [13,18–20] or knife mills [9] owing to their relatively low cost and high hardness. Boriding is an affordable diffusion-based case-hardening surface treatment for ferrous alloys to increase their hardness and wear resistance [23–25]. M42 tool steel was selected because of its combination of high hardness, high wear resistance, and adequate fracture toughness [26].

The cutters were fabricated using waterjet cutting by Definitive Solutions & Technologies, Inc (Auburn, Washington). Each cutter had an outer diameter of 115 mm and thickness of 5 mm. Bluewater Thermal Solutions (Greenville, South Carolina) performed heat treatment of all cutters and iron boriding surface treatment of the D2 cutters. Proprietary boronizing powders were used for boronizing D2 cutters. The heat treatment process was performed in a vacuum and quenched with nitrogen gas. The non-borided and borided D2 cutters were double tempered at 500°C for 2 h after quenching, whereas the M42 cutters were triple tempered at 540°C for 2 h. Representative cutters fabricated from each of the three materials are shown in Fig. 1. The apparent surface discoloration of the D2 and M42 cutters, as observed in Fig. 1b,c, is mostly cosmetic and does not affect the properties, as per discussion with the waterjet and heat treatment vendors. Vickers hardness of the cutters is listed in Table 1. The 2-body abrasive wear rate of the cutter materials also listed in Table 1 was determined by bench-scale abrasive wear testing using the standard ASTM G174 loop abrasion test [27] on test coupons. The wear rates of D2 and borided D2 coupons were reported elsewhere [9], and the wear rate of M42 steel was determined in this work using the same standard method.

2.2. Biomass feedstock

The feedstock used in shredder wear testing was high-ash corn stover, harvested from Kadolph Farm's North Field in located in Hubbard, Hardin County, Iowa, Fig. 2a. The harvest took place on October 23, 2018, using a large square baler after raking with a rotary tedder. After harvest, the bales were stored in bale form outside under a hoop shed. The fractions in the feedstock sample included cob, leaf, husk, and stalk. They were then hammer milled through a 38 mm screen. The particle size distribution of the feedstock, excluding particles smaller than 150 μm and larger than 2 mm, is shown in Fig. 2b. The feedstock had an average moisture content of 6.8 wt% and an ash content around 8 wt%.

2.3. Shredder

The experimental wear measurements were conducted using a custom-fabricated shredding unit, shown in Fig. 3. The shredder configuration consists of 42 blades: 21 blades on each side. The shafts are parallel

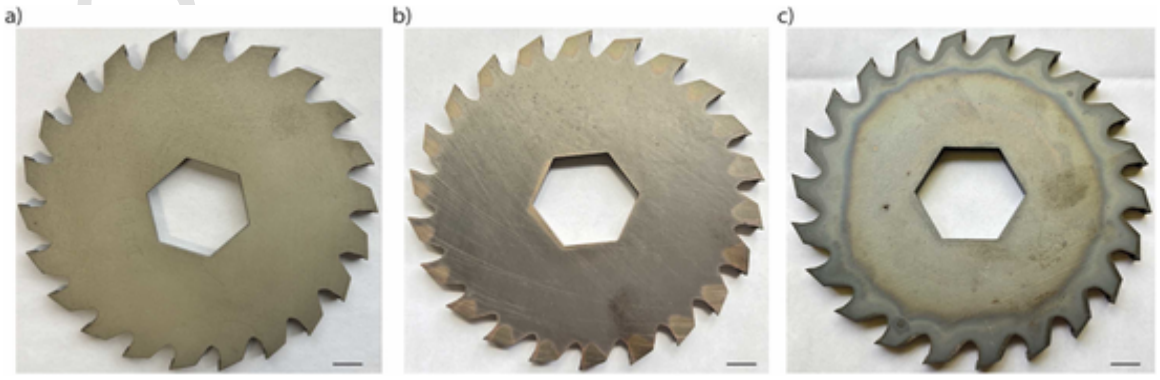

Fig. 1. Optical images of new (not tested) cutters. (a) Borided D2, (b) D2, and (c) M42 cutters. Size of the scale bar is 10 mm.

CORRECTED PROOF

Table 1
Hardness and abrasive wear properties for the selected cutter materials.

Cutter material	Hardness (HV0.05)	Abrasive wear rate ($mm^3/(N•m)$)
D2	825 ± 35	8.6×10^{-4} [9]
M42	1114 ± 70	6.7×10^{-4}
D2-borided	1411 ± 69	5.6×10^{-4} [9]

to each other, and the cutter blades overlap. The counter-rotating shafts with cutters are designed to grab and pull feedstock through a zone where the waste chips are cut, sheared, or torn into smaller pieces. During operation, the feedstock is transported to the area where the adjacent cutters overlap. The hexagonal shafts match the inner mounting holes of the cutters, locking the cutters to the shafts.

2.4. Shredder wear testing

The feedstock was fed to the shredder using a variable-speed screw system with a feed hopper at a rate of approximately 0.2 kg/min. The hopper was set at a constant feed rate of 23 Hz, and the secondary hopper ran at a rate of 60 Hz. The material was processed through the shredder at a speed of 4000 rpm. The total amount of material processed, average feed rates, and total shredding time are shown in Table 2.

2.5. Wear evaluation of cutters

The wear performance of the cutters in the shredder experiments was determined by measuring the recessive length of the cutter's tooth. The change in the cutter's tooth length over a given period during testing was measured using a digital caliper (Mitutoyo 500–196–30CAL Digimatic 0–6"/150MM W/long-form calibration; Kawasaki, Japan), with 0.01 mm resolution. The measurements were performed from the tooth base to the top edge as shown in Fig. 4. The change in the tooth length, ΔL, was determined as a difference between the initial length, $L_{initial}$, and the length at a given interval, $L_{interval}$, during testing, $\Delta L = L_{inital} - L_{interval}$. The evolving length change was measured three times on each of two teeth for each of the three cutters made from each cutter material.

2.6. Characterization of worn cutters

The morphological characterization of the cutter materials was performed using a laser digital microscope (3D Surface Profiler, VK-X3000, Keyence; Itasca, Illinois) and a scanning electron microscopy (SEM) instrument (Hitachi S4800; Japan) with an accelerating voltage of 20 kV. A metallography specimen from the borided D2 cutter was extracted using wire electrical discharge machining, mounted in epoxy, polished (finished with a 0.5 μm diamond suspension), and etched with a 2 % nital solution for microstructural for SEM characterization.

2.7. Hardness measurement

Hardness of the cutter materials was determined using Vickers and Knoop microindentation (Buehler, Model 1600 −6305) according to ASTM E384 [28]. The Vickers hardness was measured at a 50 gf load (HV0.05). Five measurements were conducted on each cutter material to determine an average value and a standard deviation as shown in Table 1. For the borided D2 cutter, the Vickers hardness was measured on the cross-section that was prepared as described in the above section. Additionally, Knoop microindentation was performed on the top surface of the borided D2 cutter sample at a 100 gf load.

2.8. Feedstock particle size analysis

The size of the corn stover particles collected during the shredder wear experiments was measured using a particle size and shape analyzer (Microtrac PartAn3D, Montgomeryville, Pennsylvania). The feret

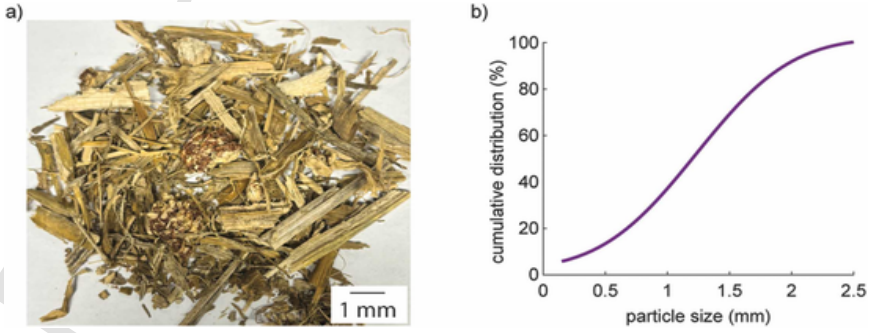

Fig. 2. Corn stover used in the shredder wear testing. (a) Optical image, (b) cumulative distribution of the particle size.

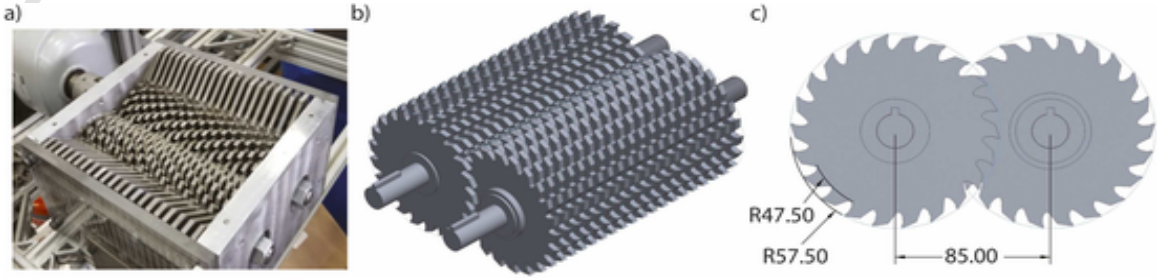

Fig. 3. A custom-built bench-scale shredder. (a) Photograph of the laboratory-scale shredder, (b) 3D computer aided assembly (CAD) of the cutter and clearing plates, and (c) layout of the adjacent cutters (all dimensions are in mm).

Table 2
Total amount of processed feedstock, average feed rate, and total shredding time for each cutter material in the shredder wear test.

Cutter material	Amount of processed feedstock (kg)	Average feed rate (g/min)	Total shredding time (hours)
D2	79	65.8	20
M42	41	85	8
Borided D2	78	65	20

width (i.e., the smallest distance between two parallel lines of a particle) was analyzed after processing 2, 30, and 80 kg of corn stover. The number of analyzed particles was in a range of 15,000 – 20,000.

3. Results and discussion

3.1. Wear performance of the cutter materials

Borided D2 cutters exhibited the highest wear resistance (the lowest wear rate) among all tested cutter materials in the shredder wear test, as determined by measuring the evolving tooth recession (Fig. 5a). At the end of the test, after processing of approximately 79 kg of feedstock, the total tooth length recession of the candidate borided D2 cutter was 0.08 mm—one-third that of the baseline D2 cutter, which experienced a recession of 0.26 mm after 78 kg of processed feedstock. Candidate M42 cutters were tested for a total of 41 kg of processed feedstock and exhibited a tooth length recession of 0.23 mm, slightly higher than the baseline D2 cutter's 0.20 mm recession after processing the same amount of feedstock. A linear fit was applied to the height recession data points for each cutter material to calculate the wear rate, defined as the cutter tooth recession in millimeters per kilogram of processed feedstock. Fig. 5b shows the tooth recession length of each cutter material during the initial period of testing.

The baseline D2 and candidate borided D2 cutters experienced two wear regimes as shown in Fig. 5a. In the first stage (running-in), at the beginning of the test, the tooth length recession was at its highest. For the baseline D2 cutters, the running-in wear rate was 8.1×10^{-3} mm/kg for the first 14 kg of processed feedstock; the wear rate then decreased to a steady-state value of 2.0×10^{-3} mm/kg, for the reminder of the shredder wear test, as shown in Table 3. For the candidate borided D2 cutters, the higher rate of the tooth length recession occurred only up to 8 kg of processed feedstock, with a running-in wear rate of 7.1×10^{-3} mm/kg. After that, the tooth recession decreased to a much lower steady-state wear rate of 2.0×10^{-4} mm/kg, which is an order of magnitude lower than that of the baseline D2 cutter.

The difference in the tooth length recession after processing 8 kg of feedstock and at the end of the test is minimal, only 0.02 mm, suggesting that the wear of the borided cutter teeth is very low once the steady-state regime is reached. In contrast to the baseline D2 and candidate borided D2 cutters, the tooth length recession of the candidate M42 cutter teeth was more linear throughout the testing period and did not slow down the wear rate after running-in.

The wear rate of the M42 cutters was more linear throughout the testing than other two types of cutters, and its transition to the steady-state wear for the M42 cutter was hardly distinguishable. Still the wear rate for the first 12 kg of processed feedstock was calculated for comparison with the D2 and borided D2 cutters, as shown in Fig. 5b. The analysis showed that the initial wear rate of the M42 cutter is 7.5×10^{-3} mm/kg, which is lower than that of the candidate D2 cutter and is similar to the borided D2 cutter, as shown in Table 3. The steady-state wear rate of the M42 cutters, which represents the total wear rate measured from the start of the test, was 5.4×10^{-3} mm/kg, which was the highest among all the studied cutter materials.

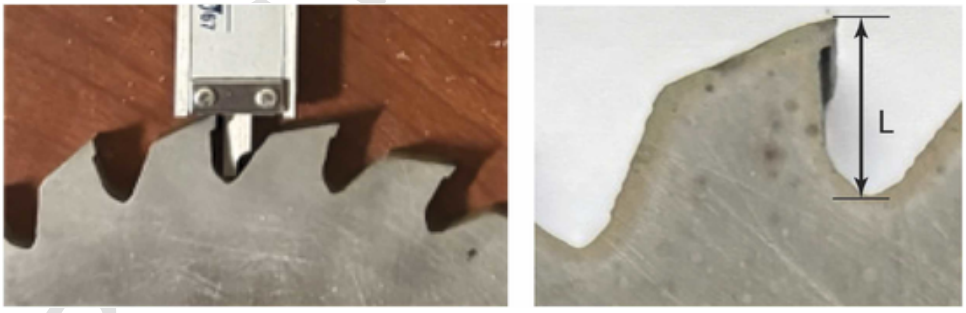

Fig. 4. Illustration of tooth length measurements where L is the length from the tooth base to the top edge.

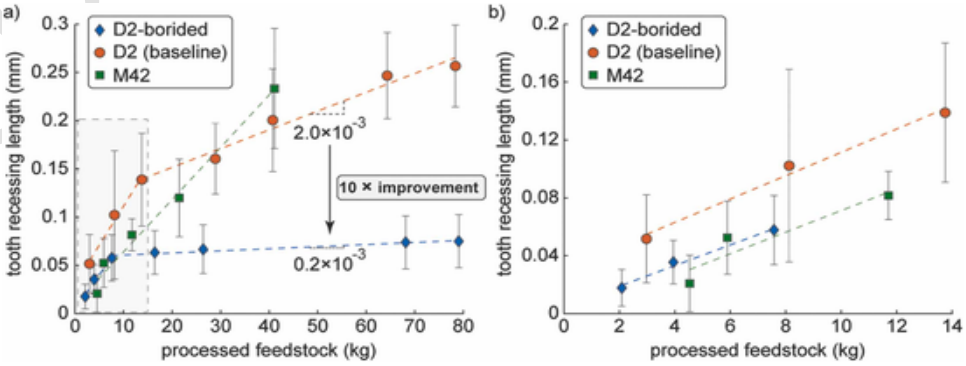

Fig. 5. Wear performance of the three cutter materials expressed as tooth recessing length for (a) the entire duration and (b) the initial period of shredder testing.

CORRECTED PROOF

Table 3
Running-in and steady-state wear rates of the cutter materials in the shredder wear tests.

Cutter material	Running-in wear rate (mm/kg)	Steady-state wear rate (mm/kg)
D2	8.1×10^{-3}	2.0×10^{-3}
M42	7.5×10^{-3}[a]	5.4×10^{-3}[a]
Borided D2	7.1×10^{-3}	2.0×10^{-4}

[a] Note: Since the transition from running-in to steady-state wear rate in M42 is indistinguishable, the running-in wear rate was determined using a linear fit up to 12 kg of processed feedstock, for easier comparison with D2 and borided D2 cutters, while the steady-state wear rate reflects the overall wear rate from the start of the shredder test.

Table 4
Identification of the primary and secondary wear modes of the cutter materials based on microstructural characterization.

Cutter material	Primary wear mode	Secondary wear mode
D2	2-body and 3-body abrasion	—
M42	2-body and 3-body abrasion	minor erosion near the tip
Borided D2	2-body and 3-body abrasion	erosion of the borided layer near the tip

3.2. Wear mechanism of the cutters

Microstructural analysis was performed to reveal the underlying wear mechanisms of the three cutter materials which are summarized in Table 4 and to determine how the boriding surface treatment of the D2 cutter enabled a 10× increase in wear resistance. Optical images of the cutters after completion of the shredder testing show that the side face of all cutter materials was subjected to combined two-body and three-body abrasive wear, which is evident from the low-magnification images in Fig. 6. The degree of the abrasive wear appears to be more severe in D2 and M42 cutters, as indicated by the visibly pronounced surface scratches shown in Fig. 6b,c.

In the candidate borided D2 cutters, the borided layer was abraded from the side face near the top edge of the tooth, as shown in Fig. 7. A higher magnification examination of the tooth morphology indicates that the transition from the borided area to the exposed substrate is relatively smooth, showing no signs of delamination or cracking, as shown in Fig. 7a–c. This observation suggests that the borided layer on the side face of the tooth tip was likely worn away by abrasion and/or erosion. The top edge of the tooth tip of the borided cutters showed evidence of chipping as a result of erosion, Fig. 7d–f.

An unworn region away from the cutting teeth, (Fig. 8a) along with one tooth of the tested D2-borided cutter (Fig. 8d) were cut out, mounted in epoxy, polished, and etched for the SEM microstructural characterization and Knoop hardness measurements. SEM images of the unworn region showed that the borided layer is fairly uniform, and the thickness is approximately 60 μm, as shown in Fig. 8b,c. The optical

E-PROOF

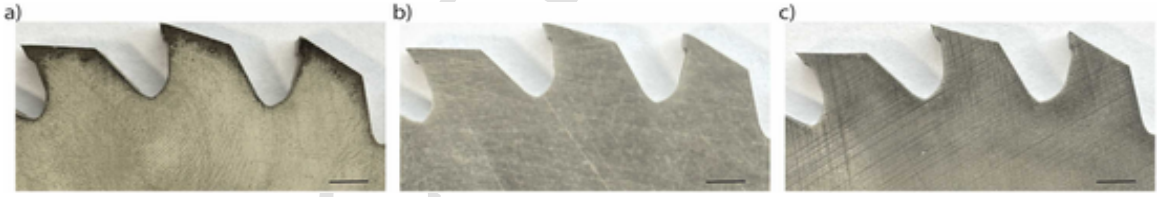

Fig. 6. Optical images of three cutters after completion of the shredder wear testing. (a) Borided D2, (b) D2, and (c) M42 cutters. Size of the scale bar is 5 mm.

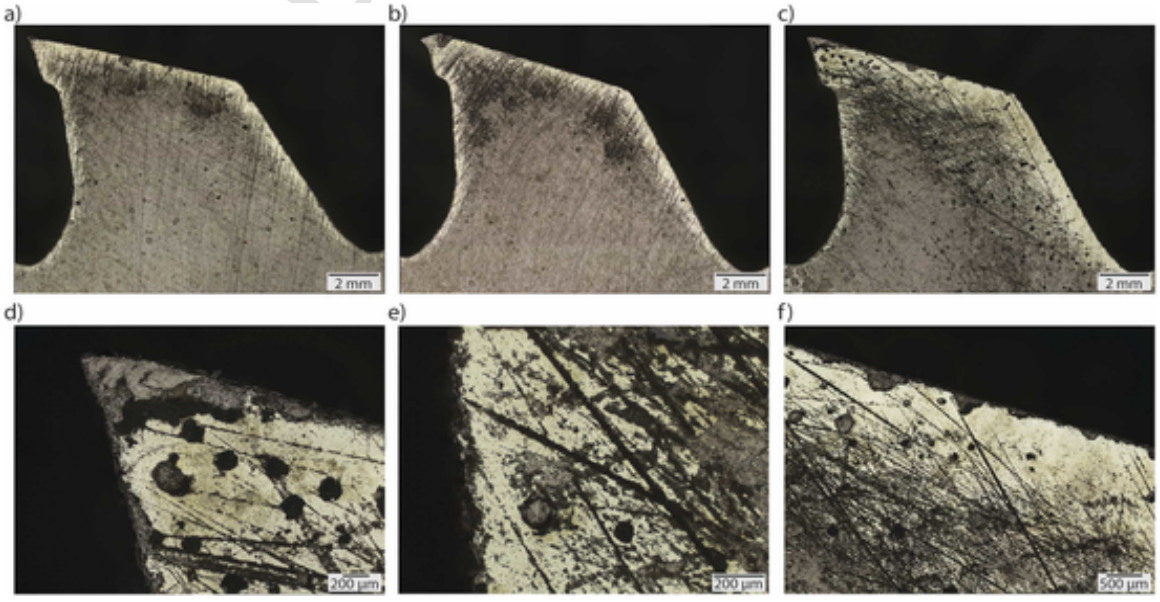

Fig. 7. Microstructural analysis of three borided D2 cutter teeth (a–c) after the completion of the shredder wear test, (d) tooth tip, (e) leading edge, and (f) top edge of the tooth shown in (c).

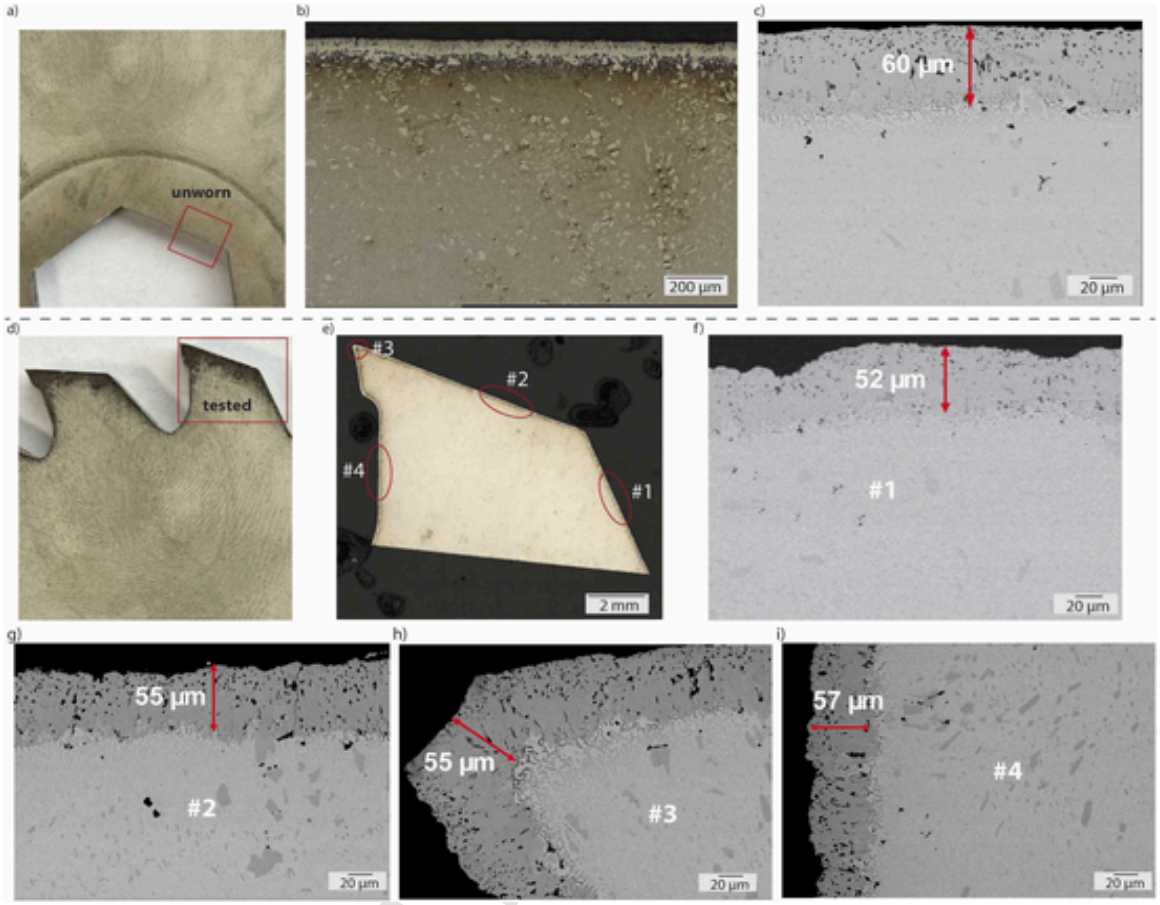

Fig. 8. Microstructural analysis of the borided layer of the D2 cutter. (a) An unworn region of the cutter that was extracted for the analysis, (b) optical and (c) SEM image showing the borided layer, (d) extracted tooth after the completion of the shredder wear testing used for the analysis, (e) optical image of the tooth showing regions of interest examined with SEM in (f–i).

and SEM images of the cutter tooth show that the borided layer was preserved on the top face of the tooth after the shredder wear test, as shown in Fig. 8d-i. Interestingly, the thickness of the borided layer was consistent across different regions along the top surface of the tooth, ranging from 52 to 57 µm (Fig. 8f-i), which is only slightly smaller than the thickness of the borided layer in the unworn cutter region.

The iron boriding surface treatment of ferrous materials could result in either a single Fe_2B or a dual FeB and Fe_2B phase [29]. A single-phase borided layer typically exhibits a sawtooth structure [24]; however, this morphology is not observed in Fig. 8. Therefore, the borided D2 cutter likely has a dual-phase borided layer. The outer FeB phase is harder and more brittle than the inner Fe_2B phase which adheres better to the substrate [24,30]. The chipping of the borided layer was only observed on the outermost surface, as observed in Fig. 8f-i, which could have been occupied by the brittle FeB phase. A formation of single-phase Fe_2B layer instead of a dual FeB and Fe_2B phase could be more desirable to resist the erosive wear and to prevent brittle failure of the borided layer.

The presence of the borided layer was also confirmed by Knoop microindentation, which revealed a steep gradient in hardness from the D2 steel substrate to the apparent borided layer, Fig. 9. The average Knoop hardness of the substrate is 1077.2 ± 110.9 and increases to 1659.8 ± 266.2 in the borided layer. The preservation of the harder borided layer and the minimal changes in its thickness after testing is in agreement with the wear measurement results, indicating that the candidate borided D2 cutters experienced minimal tooth length recession, enabling an order-of-magnitude improvement in the wear resistance in comparison to the non-treated D2 cutters .

The primary wear mode of the baseline D2 and candidate M42 cutters is combined two-body and three-body abrasion, as evident from the shorter and longer scratches on the side face, shown in Fig. 10a-c and Fig. 11a-c, respectively. A close examination of Fig. 10d-f shows that on the D2 cutter tooth the contact surface of the edges appears to be smooth (polished) with abrasive scratches parallel to each other, shown in Fig. 10d–f. In contrast, the contact surface of the edges of the cutter tooth in M42 showed signs of chipping (Fig. 11 d–f), similar to the borided D2 cutter but on a smaller scale.

3.3. Particle size distribution

Analysis of the PSD was conducted on the corn stover feedstock processed at the beginning of the testing after processing approximately 2 kg (before the cutters were worn), and after processing 30 and 80 kg of feedstock, as shown in Fig. 12. Particles smaller than 150 µm were considered to be ash or dust and were excluded from the analysis. Additionally, particles larger than 2 mm were also excluded from the analysis as they represented only a small fraction. The PSD was represented using a histogram and a cumulative distribution function. Overall, the frequency of the particles decreases with their increasing size. This trend is most notable in the D2 and borided D2 cutters, in which most the particles are smaller than 1 mm, as shown in Fig. 12a,b. Cutting with sharper, less worn cutters results in a higher frequency of smaller particles, as indicated by the cumulative distribution curves. The PSD

CORRECTED

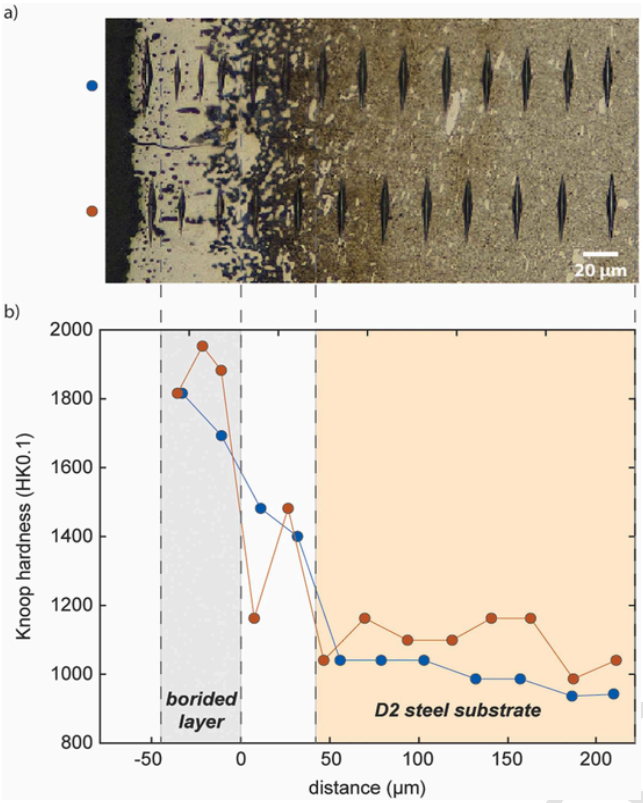

Fig. 9. Knoop microindentation results on the borided D2 cutter tooth after completion of the shredder wear test. (a) optical image, (b) hardness data.

appears to be more consistent with M42 cutters after processing 2 kg of feedstock (Fig. 12c). The PSD after processing 30 kg of feedstock showed that the frequency of the smallest particles was the lowest. This trend is the opposite of that observed with D2 and borided D2 cutters. It is not straightforward to explain the difference between the PSD of M42 cutters and those observed in D2 and borided D2. While it is plausible to assume that the higher number of smaller-sized particles at the beginning of the test in D2 and borided D2 is due to their sharper edges, it is not well understood why cutting with initially sharper M42 cutters resulted in a more even particle distribution after 2 kg of processed feedstock and fewer amount of smaller sized particles after 30 kg of processed feedstock. The PSD analysis may be influenced by the inherent measurement errors arising from the particle selection for the analysis. Although up to 20,000 particles were selected for each analysis, this number represents only a small fraction of the total processed biomass particles. Analyzing the PSD of all processed particles at each measured interval would be highly time-consuming and impractical.

3.4. Relationship between the cutter materials and the wear performance

The results of the shredder wear testing clearly demonstrated that the boriding surface treatment improved the wear resistance of the baseline D2 tool steel cutters. The improvement in the wear resistance could be contributed to the higher hardness of the borided layer. A 1.7× increase in the cutter hardness resulted in 10× improvement in wear resistance. The effect of the boriding surface treatment is especially notable in the transition from the initially higher running-in wear to a lower steady-state wear as the shredding test progresses.

Microstructural analysis showed that the primary wear mode in all three cutter materials is abrasion. In addition to the higher hardness, boriding surface treatment also increased the abrasive wear resistance of the D2 tool steel, as determined by a loop abrasion test, the results of which are listed in Table 1. Therefore, the high abrasive wear resistance of the borided surface treatment is responsible for the significant improvement of the wear performance of the D2 cutters. However, the high hardness of the borided layer comes at the cost of lower fracture toughness, which is evident from the chipping of the top surface in the

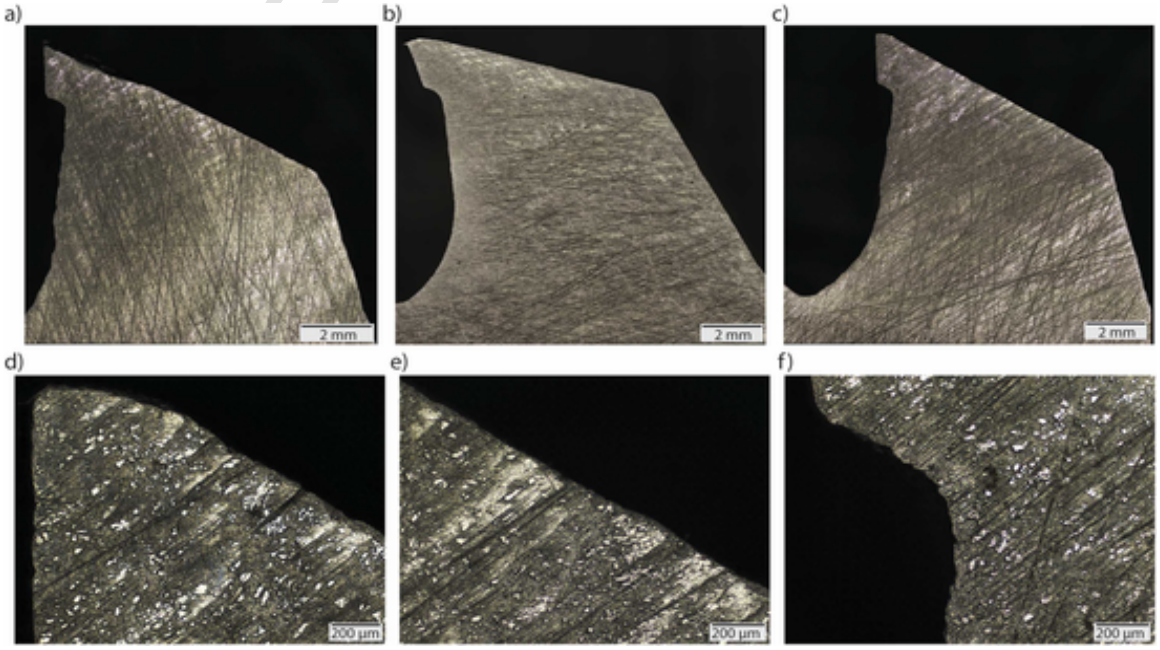

Fig. 10. Microstructural analysis of three D2 cutter teeth (a–c) after completion of the shredder wear test, (d) tooth tip, (e) leading edge, and (f) top edge of the tooth shown in (c).

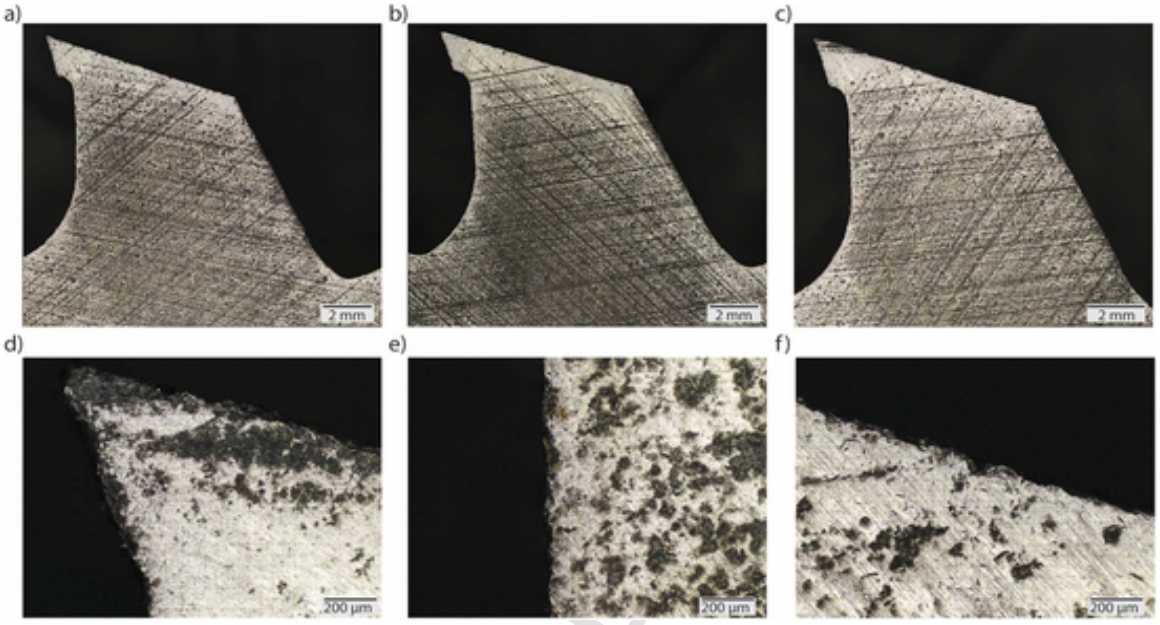

Fig. 11. Microstructural analysis of three M42 cutter teeth (a–c) after completion of the shredder wear test, (d) tooth tip, (e) leading edge, and (f) top edge of the tooth shown in (c).

D2 borided layer, as shown in Fig. 7. The surface damage and chipping of the borided layer may have occurred during the initial stage of the shredder wear test, when the cutter edge was the sharpest, owing to higher contact stresses between the feedstock particles and the cutter edge. The evolution of the wear of the borided D2 cutter in Fig. 5a showed that its wear rate was the highest during the initial period. At the end of the test, the hard and wear-resistant borided layer was still present at the edge of the cutter's tooth, suggesting that the softer D2 steel substrate was protected from the abrasive wear and that the borided layer greatly contributed to the overall improved wear resistance of the D2 cutters.

The softer D2 cutter teeth have higher fracture toughness, and the shredder wear testing did not cause chipping of the cutter's tooth edge. The polished appearance of the edge surface is due to abrasion. Because the abrasive wear is the dominant wear mechanism of the cutters in the shredder, the poor performance of the D2 cutter is due to its lower hardness and lower abrasive wear resistance. A transition from an initially higher wear rate to a lower steady-state wear rate in the D2 and borided D2 cutters could be attributed to the geometric changes at the cutter edge which evolved during the processing of the biomass feedstock. As the abrasion thickened and blunted the edge, the contact pressure decreased, potentially significantly reducing the wear rate.

Curiously, the evolution of the wear in the candidate M42 alloy appears to be linear and no transition from the running-in to the steady-state wear regime was observed. Although the initial wear rate was less than that of the D2 cutters, the final measured data point after processing 41 kg of feedstock showed more wear. It was expected that the wear rate of the M42 cutter would eventually decrease as the edge became thicker and blunter due to abrasive wear, which is a hypothesized wear mechanism in the D2 and borided D2 cutters. The reason that the M42 cutters did not transition to a lower steady-state wear rate remain unclear at this moment and warrant future investigation. For the D2 cutters, the dominant wear mode is two-body and three-body abrasion and the wear rate of the cutters eventually decreased due to the blunting the of the edge. For the borided D2 cutters, the high hardness and abrasion resistance of the borided layer were sufficient to minimize the two-body and three-body abrasive wear as well as erosion of the cutter's tip, after the initial blunting. Failure of M42 to achieve a lower steady-state wear rate could be due to combined action of abrasion and erosion at the cutter's edge. Microstructural characterization in Fig. 11 revealed that the primary wear mechanism in M42 cutters is a two-body and three-body abrasion and a minor erosion near the tip. The higher hardness and decreased fracture toughness resulted in erosive wear at the tooth edge but to a lower degree than in the borided D2 layer. However, the higher hardness of the M42 seemed to be beneficial only during the initial stage of the shredder testing in which the wear rate was lower than that of the D2 cutter. It is hypothesized that continuous erosive wear caused by decreased fracture toughness was responsible for the higher wear of M42 after the running-in period. Although the cutter's edge becomes blunter as abrasive wear progresses, the wear may have remained at higher rates due to continuous erosion caused by dynamic contact with the hard and abrasive inorganic contaminants present in the biomass feedstock.

There is a possibility that the wear rate of the M42 cutters could have transitioned to a lower steady state if the shredder testing continued further, similar to the other two cutter materials. However, the shredder wear testing of the M42 cutters did not progress beyond processing 41 kg of feedstock, because the preliminary measurements of the wear rate indicated they already had a higher wear loss compared with the baseline D2 cutters by then.

Enhanced wear resistance is not the only factor that needs to be considered for selecting a candidate cutter material. Because biomass preprocessing is an industry-driven field, the operational costs play a crucial role in material selection. Although, in this case, the boriding surface treatment improved the durability of the cutters, the cost of the cutter would be higher. Therefore, a TEA must be conducted to clarify the economic benefits from utilizing more wear-resistant, but costlier, cutter materials. Several factors should be taken into consideration, including the cost of the material, overall improvement of the cutter durability, downtime cost owing to cutter replacement, and power consumption. TEA analysis of a knife mill operation by Grejtak et al. [9] showed that the higher cost associated with the boriding surface treatment for tool steel knives and WC as a bulk overlay of steel knives resulted in an overall lower milling operation cost and reduced power consumption. Although TEA was not performed in this study because of a lack of key inputs, the significant improvement in the wear resistance

CORRECTED P

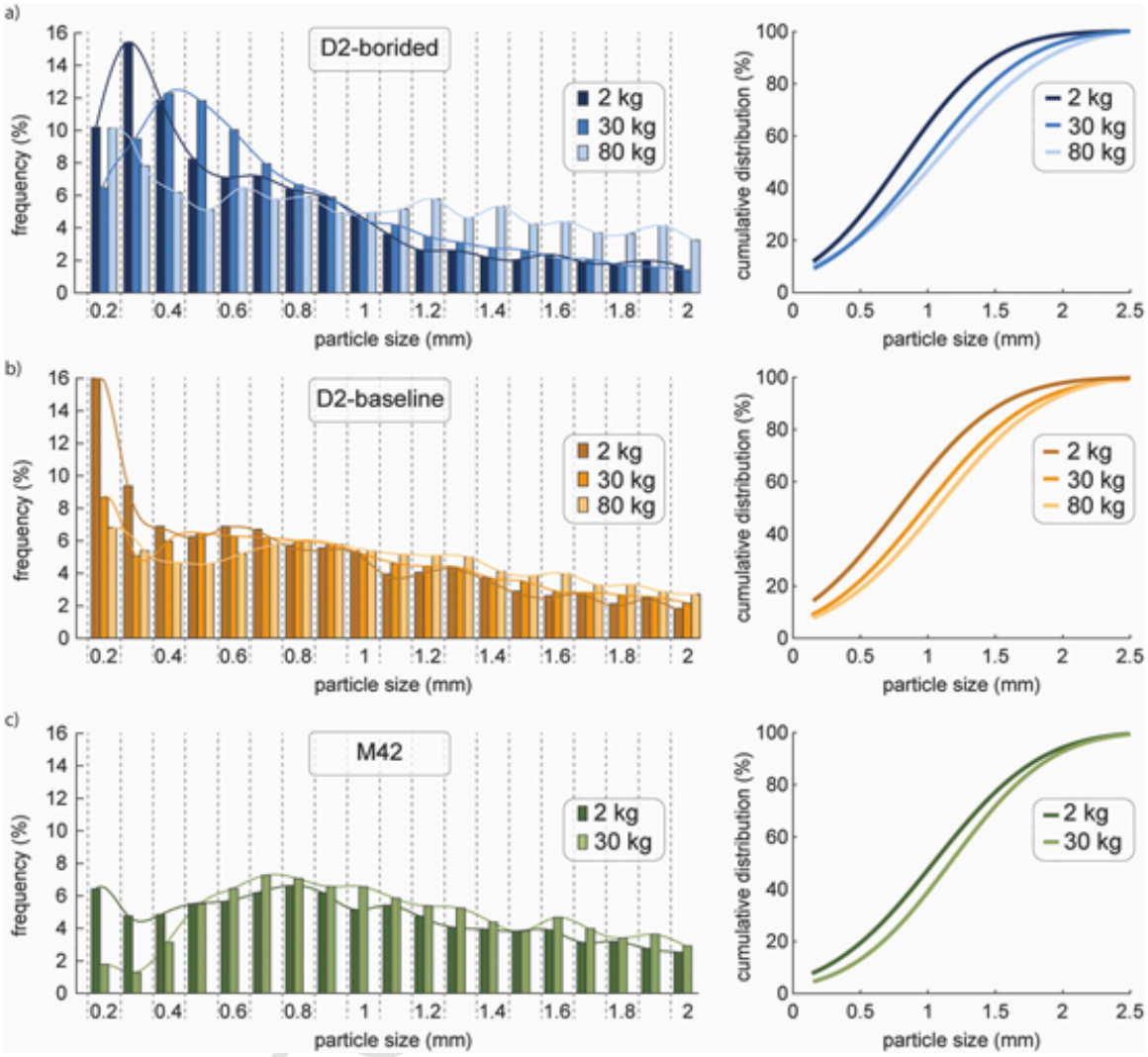

Fig. 12. Histograms of the particle size distribution and corresponding cumulative distribution curves of (a) borided D2, (b) D2, and (c) M42 cutters after completion of the shredder wear testing.

of the borided D2 cutters suggests that the boriding surface treatment could be an economically feasible option for enhancing cutter durability and reducing operational costs.

4. Conclusions

This study examined the wear performance of three cutter materials: D2 tool steel as the baseline, iron borided D2 tool steel as a candidate for surface treatment, and M42 tool steel as a candidate alloy using a shredder test for size reduction of a high-ash corn stover feedstock. The shredder wear testing demonstrated that the iron boriding improved the wear resistance by one order of magnitude. All three cutter materials showed a higher wear at the beginning of the shredder test; but the D2 and borided D2 cutters transitioned to lower steady state afterward. The borided D2 exhibited the lowest steady-state wear rate among all three cutter materials. The improvement in the wear resistance was enabled by a high hardness and abrasive wear resistance of the borided layer, which was still present on the cutter after completion of the shredder testing. The higher hardness of the M42 appeared to provide benefits only during the initial stage of shredder testing. The dominant wear modes in all three cutter materials were identified as a two-body and three-body abrasion. Erosive wear was also observed on the edge of the borided layer. Future studies are to investigate the feasibilities of other surface treatment methods for biomass size reduction tools.

CRediT authorship contribution statement

Qu Jun: Writing – review & editing, Supervision, Resources, Project administration, Methodology, Investigation, Funding acquisition, Formal analysis, Conceptualization. **Blau Peter J.:** Writing – review & editing, Investigation. **Fenske George:** Supervision. **Ajayi Oyelayo O.:** Writing – review & editing, Supervision, Investigation. **Lacey Jeffrey A.:** Writing – review & editing, Supervision, Resources, Methodology, Investigation, Funding acquisition, Conceptualization. **Kuns Miranda W.:** Writing – review & editing, Investigation, Formal analysis, Data curation. **Grejtak Tomas:** Writing – original draft, Visualization, Methodology, Investigation, Formal analysis, Data curation.

Declaration of competing interest

The authors declare that they have no known competing financial interests or personal relationships that could have appeared to influence the work reported in this paper.

CORRECTED

Acknowledgments

The authors would like to thank Craig Zimmerman from Bluewater Thermal Solutions for conducting heat treatment and boriding of the steel cutters and for thoughtful comments and insight. The authors would like to acknowledge Daniel Fleming and Caitlin Duggan from Oak Ridge National Laboratory for sample preparation. This research was sponsored by the Feedstock Conversion Interface Consortium of the Bioenergy Technologies Office, Office of Energy Efficiency and Renewable Energy, US Department of Energy .

Notice: This manuscript has been authored by UT-Battelle, LLC, under contract DE-AC05–00OR22725 with the US Department of Energy (DOE). The US government retains and the publisher, by accepting he article for publication, acknowledges that the US government retains a nonexclusive, paid-up, irrevocable, worldwide license to publish or reproduce the published form of this manuscript, or allow others to do so, for US government purposes. DOE will provide public access to these results of federally sponsored research in accordance with the DOE Public Access Plan Access Plan (http://energy.gov/downloads/doe-public-access-plan).

Data availability

Data will be made available on request.

References

[1] Kratky L, Jirout T. Biomass size reduction machines for enhancing biogas production. Chem Eng Technol 2011;34:391–9.
[2] Oyedeji O, Gitman P, Qu J, Webb E. Understanding the impact of lignocellulosic biomass variability on the size reduction process: a review. ACS Sustain Chem Eng 2020;8:2327–43.
[3] Colley Z, Fasina O.O, Bransby D, Lee Y.Y. Moisture effect on the physical characteristics of switchgrass pellets. Trans ASABE 2006;49:1845–51.
[4] Lisowski A, Matkowski P, Dąbrowska M, Piątek M, Świętochowski A, Klonowski J, Mieszkalski L, Reshetiuk V. Particle size distribution and physicochemical properties of pellets made of straw, hay, and their blends. Waste Biomass-- Valoriz 2020;11:63–75.
[5] Shen J, Wang X.-S, Garcia-Perez M, Mourant D, Rhodes M.J, Li C.-Z. Effects of particle size on the fast pyrolysis of oil mallee woody biomass. Fuel 2009;88:1810–7.
[6] Gómez N, Banks S.W, Nowakowski D.J, Rosas J.G, Cara J, Sánchez M.E, Bridgwater A.V. Effect of temperature on product performance of a high ash biomass during fast pyrolysis and its bio-oil storage evaluation. Fuel Process Technol 2018;172:97–105.
[7] Chaloupková V, Ivanova T, Ekrt O, Kabutey A, Herák D. Determination of particle size and distribution through image-based macroscopic analysis of the structure of biomass briquettes. Energies (Basel) 2018;11:331.
[8] Ohgren K, Rudolf A, Galbe M, Zacchi G. Fuel ethanol production from steam-pretreated corn stover using SSF at higher dry matter content. Biomass Bioenergy 2006;30:863–9.
[9] Grejtak T, Lacey J.A, Kuns M.W, Hartley D.S, Thompson D.N, Fenske G, Ajayi O.O, Qu J. Improving knife milling performance for biomass preprocessing by using advanced blade materials. Wear 2023;204714.
[10] Bitra V.S.P, Womac A.R, Igathinathane C, Sokhansanj S. Knife mill comminution energy analysis of switchgrass, wheat straw, and corn stover and characterization of particle size distributions. Trans ASABE 2010;53:1639–51.
[11] Naimi L.J, Sokhansanj S, Bi X, Lim C.J, Womac A.R, Lau A.K, Melin S. Development of size reduction equations for calculating energy input for grinding lignocellulosic particles. Appl Eng Agric 2013;29:93–100.
[12] Roy S, Lee K, Lacey J.A, Thompson V.S, Keiser J.R, Qu J. Material characterization-based wear mechanism investigation for biomass hammer mills. ACS Sustain Chem Eng 2020;8:3541–6.
[13] Lee K, Lanning D, Lin L, Cakmak E, Keiser J.R, Qu J. Wear mechanism analysis of a new rotary shear biomass comminution system. ACS Sustain Chem Eng 2021;9:11652–60.
[14] Lacey J.A, Aston J.E, Thompson V.S. Wear properties of ash minerals in biomass. Front Energy Res 2018;6:1–6.
[15] J.A. Lacey, J.E. Aston, S. Hernandez, V.S. Thompson, M.S. Intwan, K. Lee, J. Qu, "Wear and Why? How Ash Elements Can Help Define Wear Profiles of Biomass Feedstocks" In: *American Society of Agricultural and Biological Engineers*; 2019. doi: 10.13031/aim.201901446
[16] Lee K, Roy S, Cakmak E, Lacey J.A, Watkins T.R, Meyer H.M, Thompson V.S, Keiser J.R, Qu J. Composition-preserving extraction and characterization of biomass extrinsic and intrinsic inorganic compounds. ACS Sustain Chem Eng 2020;8:1599–610.
[17] Blau P.J, Grejtak T, Qu J. The characterization of wear-causing particles and silica sand in particular. Wear 2023;530–531:204872.
[18] Fenske G, Ajayi O, Lin L, Qu J, Lanning D. Analysis of Cutter Blade Wear in Rotary Shear Mills. Argonne, IL (United States): Argonne National Laboratory (ANL); 2022.
[19] Lin L, McKiernan C, Lanning D, Keiser J.R, Qu J. Contact pressure analysis to allow improved design for the clearing plate in a biomass comminution system. Biomass Convers Biorefin 2023;1–7.
[20] Lin L, Lanning D, Keiser J.R, Qu J. Investigation of cutter–woodchip contact pressure in a new biomass comminution system. Front Energy Res 2022;10:754811.
[21] Davis J.R. Surface Engineering for Corrosion and Wear Resistance. ASM international; 2001.
[22] Hoornaert T, Hua Z.K, Zhang J.H. Hard wear-resistant coatings: A review. In: Luo J, Meng Y, Shao T, Zhao Q, editors. Advanced Tribology. Springer; 2010. p. 774–9.
[23] Pugacheva N.B, Trushina E.B, Bykova T.M. Research on the tribological properties of iron borides as diffusion coatings. J Frict Wear 2014;35:489–96.
[24] Zimmerman C. Boriding (Boronizing) of Metals. Steel Heat Treating Fundamentals and Processes. ASM International; 2013. p. 709–24.
[25] Martini C, Palombarini G, Poli G, Prandstraller D. Sliding and abrasive wear behaviour of boride coatings. Wear 2004;256:608–13.
[26] Hudson Tool Steel Corp., ⟨https://www.hudsontoolsteel.com/technical-data/steelM4⟩.
[27] A. G174-04. Standard test method for measuring abrasion resistance of materials by abrasive loop contact. ASTM Annual Book of Standards 2014;3:735–9.
[28] Standard test method for Knoop and Vickers hardness of materials, ASTM E384, ASTM Standards, W. Conshohocken, PA, 2010.
[29] Zimmerman C. Boriding (Boronizing) of Metals. Steel Heat Treating Fundamentals and Processes. ASM International; 2013. p. 709–24.
[30] Pakseresht A, Mosas K.K.A. Coatings for High-Temperature Environments: Anti-Corrosion and Anti-Wear Applications. Springer Nature; 2023.

CORRECTED PROOF